Impact of Phase Noise in Full Duplex Wireless Systems

Keerthi Priya Dasala
Department of Electrical and Computer Engineering
Rice University, Houston, Texas - 77005
Email: keerthi.dasala@rice.edu

***Abstract*—Recent experimental results have shown that full-duplex communication is possible for short-range communications. However, extending full-duplex to long-range communication remains a challenge, primarily due to residual self-interference, even with a combination of passive suppression and active cancelation methods. A detailed study is first done to classify all known full-duplex architectures based on how they compute their canceling signal and where the canceling signal is injected to cancel self-interference. Based on the classification, various methods are analysed to identify the bottlenecks in the system performance. The key bottleneck in current systems turns out to be the phase noise in the local oscillators in the transmit-and-receive chain of the full-duplex node. In this project, the analysis of oscillator phase noise effects on the self-interference cancellation capability of full-duplex direct-conversion radio transceivers is studied in detail. Phase noise is studied to understand what limits the amount of active analog cancellation in a full duplex system design, how do the number of cancelations by active analog and digital cancelers depend on each other in a cascaded system and finally how and when passive suppression impact the amount of active analog cancelation. In addition, an example case is studied to see the impact of phase-noise in single-input-single-output(SISO) full-duplex orthogonal frequency division multiplexing (OFDM) system which can be later extend to multiple-input-multiple-output(MIMO) system.**

I. Introduction

In full-duplex communication, a node can simultaneously transmit one signal and receive another signal on the same frequency band. The key challenge in full-duplex communications is self-interference, which is the transmitted signal being added to the receive path of the same node. Due to the proximity of the transmit and receive antennas on a node, self-interference is often many orders of magnitude larger than the signal of interest. Thus, the main objective for full-duplex design is to reduce the strength of self-interference as much as possible, i.e., ideally, down to the noise floor [5].

In practical designs of full-duplex [1-9], self-interference is managed by reducing it by a combination of passive and active techniques. Passive methods rely on increasing the pathloss between the transmitter and receiver on the full-duplex node. Active cancellation techniques employ the knowledge of self-interference and inject a cancelling signal to create a null for the self-interference signal. However, experimental observations report that practical designs to date do not eliminate the self-interference completely. In fact [2] reports that strength of the residual self-interference even after passive and active cancellation is used is about 15 dB higher than the thermal noise floor.

Active cancelation can occur before or after analog-to-digital conversion. If active cancelation occurs prior to digitization of the received signal, it is referred to as active analog cancelation. The cancelation that operates on the received signal in digital baseband is labeled digital cancelation.

In this project, a detailed study is done to first classify all known full-duplex architectures based on how they compute their canceling signal and where the canceling signal is injected to cancel self-interference. Based on the classification, various methods are analysed to identify the bottlenecks in the system performance . Transmitter phase noise, receiver phase noise, in-phase/ quadrature (IQ) imbalance, power amplifier nonlinearity, and quantization noise are some of the impairments in the transmit receive chain at the full-duplex node, which can possibly limit the amount of active analog cancelation [5]. If a 14-bit analog-to-digital converter (ADC) is used, which delivers a signal-to-quantization noise ratio of 84 dB, making quantization noise much smaller than the thermal noise, thus ruling quantization noise out as a source of bottleneck in estimation of self-interference and, consequently, active analog cancelation. IQ imbalance does not significantly vary with time and can be easily calibrated, thus eliminating it as a source of bottlenecks. The power amplifier shows significant nonlinearity only when it is operated in its nonlinear regime. This leads to the implication that the key bottleneck in current systems turns out to be the phase noise in the local oscillators in the transmit-and-receive chain of the full-duplex node.

In this project, the analysis of oscillator phase noise effects on the self-interference cancellation capability of full-duplex direct-conversion radio transceivers is studied in detail. Phase noise is studied(not limited to) to understand what limits the amount of active analog cancellation in a full duplex system design, how do the number of cancelations by active analog and digital cancelers depend on each other in a cascaded system and finally how and when passive suppression impact the amount of active analog cancelation [5].

In addition, an example case is studied to see the impact of phase-noise in single-input-single-output(SISO) full-duplex orthogonal frequency division multiplexing (OFDM) system which can be later extend to multiple-input-multiple-output(MIMO) system.

II. Reducing Self-Interference in Full Duplex

A. Need for Self-Interference Reduction

A node operating in full-duplex receives a combination of a signal of interest and a self-interference signal. The physical proximity of transmit-and-receive antennas causes the self-interference signal to be 50-100 dB stronger than the signal of interest. The received signal is processed in digital baseband only after it is digitized. Prior to digitization, the automatic gain control (AGC) scales the input to a nominal range of [-1, 1]. The strong self-interference signal governs the gain control settings of the AGC, which results in the weak signal of interest occupying a range much smaller than [-1, 1] in the quantized signal.

After digitization, even if the self-interference signal can be perfectly subtracted out, quantization noise in the signal of interest will be significantly large, leading to a very low effective SNR in digital baseband. Thus, it is necessary to reduce the strength of the self-interference signal prior to the digitization of the received signal so that the signal of interest has a better effective SNR in digital baseband. In this Section, first a mathematical model is developed to describe the received signal at the full-duplex node in the "conventional" sense and then analyse the limit of the amount of active cancellation due to estimation error. It is observed that the estimation error does not satisfactorily explain limitations in active cancellation observed from experimental data in [1, 2].

B. Methods of Reducing Self-Interference

Self-interference is reduced by both passive and active techniques. Following is a brief review of the methods to reduce self-interference, whose diagrammatic classification is shown in Fig. 1.

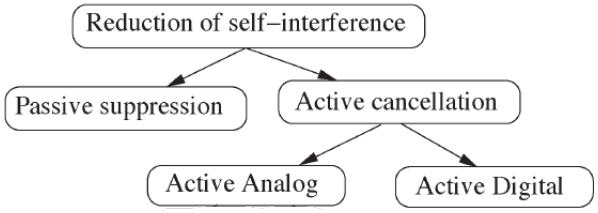

Fig. 1. Classification of methods of reducing self-interference [5]

1) Passive Suppression: Passive suppression reduces the strength of self-interference prior to it impinging upon the receive antenna by reducing the electromagnetic coupling between the transmit and receive antennas at the full-duplex node (see Fig. 2). Passive methods include 1) antenna separation,2) directional separation, 3) decoupled antenna, 4) polarization decoupling 5) circulator isolation.

2) Active Analog Cancellation: Actively reducing selfinterference by injecting a canceling signal into the received signal in the analog domain is referred to as active analog cancelation. As shown in Fig. 2, active analog cancelation operates on the received signal that has already been suppressed via passive suppression. The objective of active analog cancelation

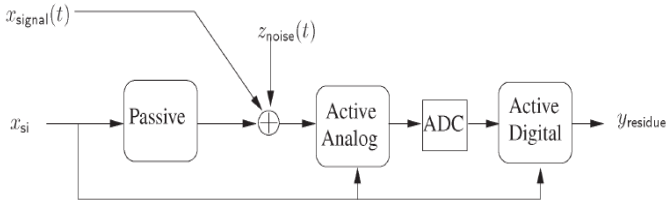

Fig. 2. Block diagram representation of all the self-interference reduction methods in concatenation[5].

is to create a null for the self-interference signal, which can be done either at the carrier frequency (i.e., RF) or at the analog baseband. Most active analog cancelers cancel self-interference at RF.

a) Active analog cancellation at RF: In Fig. 3(a), a block diagram is shown of an active analog canceler that cancels at RF. Note that, if the cancelation has to be performed at RF, then the canceling signal also needs to be upconverted to RF. The canceling signal is generated by processing the self-interference signal $x_{si}(t)$. The active analog cancelers are classified based on whether the canceling signal has been generated by processing the self-interference signal $x_{si}(t)$ prior or after upconversion. Those cancelers where the canceling signal is generated by processing $x_{si}(t)$ prior to upconversion are called pre-mixer cancelers, whereas cancelers where the canceling signal is generated by processing after $x_{si}(t)$ is upconverted are called postmixer cancelers. Fig. 3(a) shows pre-mixer processing function $f(\cdot)$ and post-mixer processing function $g(\cdot)$. Functions $f(\cdot)$ and $g(\cdot)$ are ideal if they completely eliminate self-interference from the received signal.

b) Baseband analog canceler: An active analog canceler where the canceling signal is generated in baseband and the cancelation occurs in the analog baseband is called a baseband analog canceler. Fig. 3(b) shows a representation of the baseband analog canceler. In baseband analog cancelers, selfinterference signal $x_{si}(t)$ is processed by function $s(\cdot)$, either in the baseband analog domain or in the digital domain, before it is added to the received signal to perform the cancelation. Since the canceling signal does not go through the upconversion process, possibly less RF hardware is required to implement it.

3) Digital Cancellation: The active cancelation that occurs in the digital domain after the received signal has been quantized by an analog-to-digital converter (ADC) is called active digital cancelation.

III. Reducing Self-Interference via Active Cancelation

A. Conventional System model for Self-Interference

The focus is mainly on narrowband SISO full-duplex systems. Let N1 denote the full-duplex node and N2 denote the node from which N1 is receiving a signal-of-interest. Let $x_{si}(t)$ and $x_s(t)$ denote the self interference signal and signal-of-interest. For a narrowband SISO channel, we can assume that the self-interference channel at node N1 is modeled

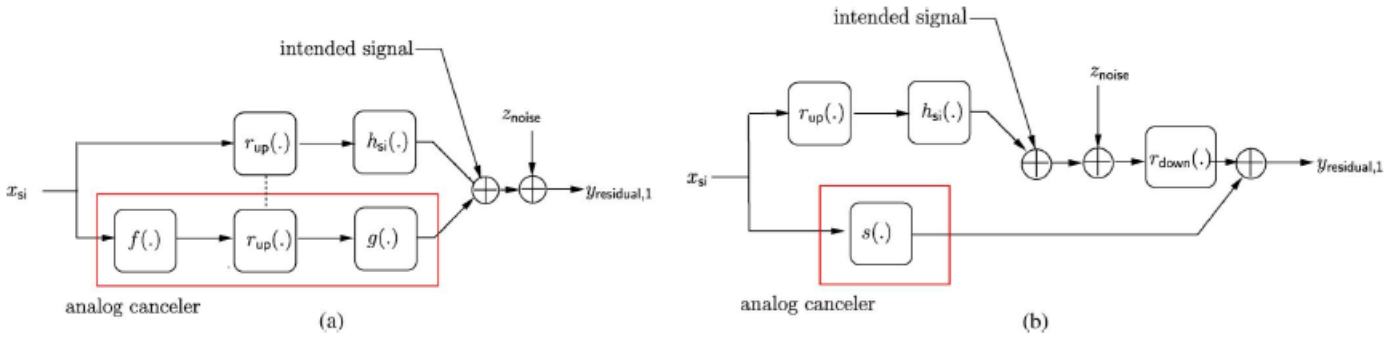

Fig. 3. Block diagram representation of all the self-interference reduction methods in concatenation.[5]

as a single delay tap channel and is denoted by $\boldsymbol{h}_{si}(t) = h_{si}\delta(t-\Delta_{si})$, where $h_{si} \in C$ is attenuation and $\Delta_{si} \in R^+$ is the delay after which the self-interference signal $x_{si}(t)$ arrives at the receiver. Similarly, the channel from the transmitter of N2 to the receiver of N1 is denoted by $\boldsymbol{h}_s(t) = h_s\delta(t-\Delta_s)$,, where $h_s \in C$ and $\Delta_s \in R^+$. The received signal at node N1, $y(t)$, is a combination of the self-interference signal and the signal-of- interest and is given by

$$y(t) = h_{si}x_{si}(t-\Delta_{si}) + h_s x_s(t-\Delta_s) + z(t) \quad (1)$$

where z(t) is the receiver thermal noise with $N(0,\sigma^2)$ distribution. The transmit power constraints at nodes $N1$ and $N2$ are described by

$$\mathbb{E}(|x_{si}(t)^2) \leq 1; \mathbb{E}(|x_s(t)^2) \leq 1 \quad (2)$$

B. Impact of Estimation Error on Active Cancellation

Given an estimate of the self-interference channel, $\hat{\boldsymbol{h}}_{si}(t) = \hat{h}_{si}(t-\hat{\Delta}_{si})$, a cancelling signal, $x_c(t) = \hat{h}_{si}x_{si}(t-\hat{\Delta}_{si})$ can be generated. Adding the cancelling signal to the received self-interference signal results in a residual

$$y_{res}(t) = h_{si}x_{si}(t-\Delta_{si}) - \hat{h}_{si}x_{si}(t-\hat{\Delta}_{si}) + z(t) \quad (3)$$

Let a training sequence $[s_1, s_2, ...s_{train}]$ of length T_{train} , with $\mathbb{E}(|x_{si}(t)^2) \leq 1$, where $i \in \{1, 2, ..., T_{train}\}$ be used to obtain the estimate, $\hat{h}_{si}(t)$ of the self-interference channel. Then, it can be shown

$$\mathbb{E}(|y_{res}|^2) < \frac{5\sigma_z^2}{T_{train}} + \sigma_z^2 \quad (4)$$

According to (4), the residual should decay inversely with the length of training sequence and even with a very short training length, say $T_{train} = 5$, the residual self-interference is no more than 3 dB above thermal noise.It is observed that the residual self-interference is 15 dB higher than the thermal noise which is clearly not explained by the signal model in (1), raising a possibility of some other source of impairment leading to a bottleneck in active cancellation.

IV. Identifying Phase Noise as Bottleneck in Cancellation

A. Active Cancelation

In this section, the bottleneck in active cancellation observed in [1, 2] is identified by measuring the amount of active cancellation in a controlled experiment as shown in Fig.4

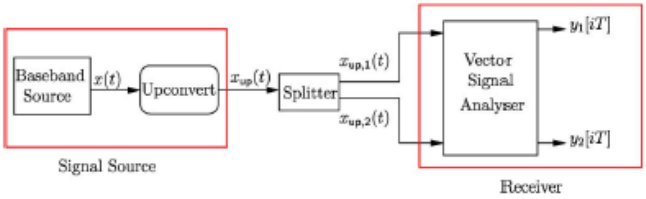

Fig. 4. Schematic of the experiment in [1,2]

The transmitted signal, $x[iT]$, is narrowband,where $i \in \mathbb{Z}$ and T is the sampling rate.Therefore if the upconversion process does not add any noise, then the received sequences can be written as

$$y_1[iT] = h_1 e^{-j(w_c+w)\Delta_1}x[iT] + z_1[iT] \quad (5)$$
$$y_2[iT] = h_2 e^{-j(w_c+w)\Delta_2}x[iT] + z_2[iT] \quad (6)$$

where h_1 and h_2 are complex attenuations. Since the signals only travel over a wire, the attenuations hI and h2 can be assumed to be constant. Note that, $y_1[iT]$ and $y_2[iT]$ are noisy versions of same signal, $x[iT]$, scaled by different quantities. Therefore, we can mimic active cancellation by subtracting a scaled and delayed version of the $y_1[iT]$ from $y_2[iT]$. The residual after active cancellation will be

$$y_{res,d}(iT) = y_2[iT] - h(d)y_1[(i-d)T] \quad (7)$$

where $d \in \mathbb{Z}$ is the delay in the number of samples, and $h(d)$ is the scaling as a function of the delay. Using $N \in \mathbb{N}$ samples of the received sequences $y_1[iT]$and $y_2[iT]$, the scaling is computed as

$$h(d) = \frac{\sum_{i=1}^{N} y_2[iT]' y1[(i-d)T]}{\sum_{i=1}^{N} |y_2[iT]|^2} \quad (8)$$

As $N \to \infty$

$$\mathbb{E}(|y_{res,d}[iT]|^2) = \frac{|h_1|^2}{|h_2|^2}\sigma_z^2 + 2\sigma_z^2 \quad (9)$$

For the experiment conducted $\frac{|h_1|^2}{|h_2|^2} \approx 1$, thus it is expected that strength of the residual self-interference should be approximately $3\sigma_z^2$ a quantity independent of the delay d.

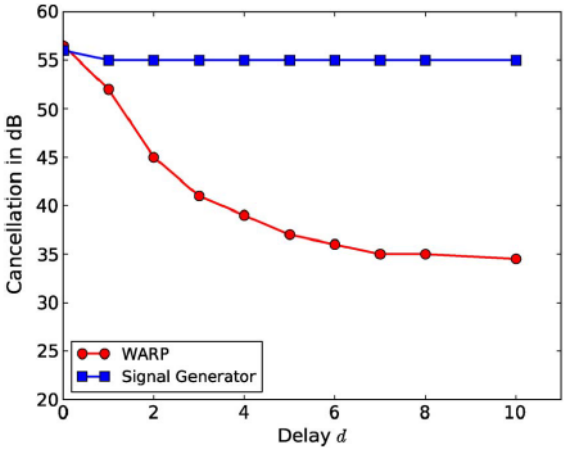

Fig. 5. Amount of cancelation as a function of the delay for different signal sources measured from the experiment in Section IV [5]

The resulting strength of the residual self-interference is

$$\mathbb{E}(|y_{res,d}[iT]|^2) = 2|h_1|^2\sigma_\phi^2(1 - R_\phi(dT)) + 2\sigma_z^2$$

As the delay increases, it is natural that the temporal correlation in phase noise reduces. Therefore the amount of cancellation, when WARP is used as a signal source, will reduce as the delay increases which explains the trend of cancellation in the experiments. Once the delay is sufficiently large, $R_\phi(dT)) \approx 0$, thus the dependence of the residual on delay will vanish.Thus, the lower bound due to phase noise is close to upper bound of cancellation due to dynamic range limitations of the VSA, thus there is no apparent variation in active cancellation with varying delay.

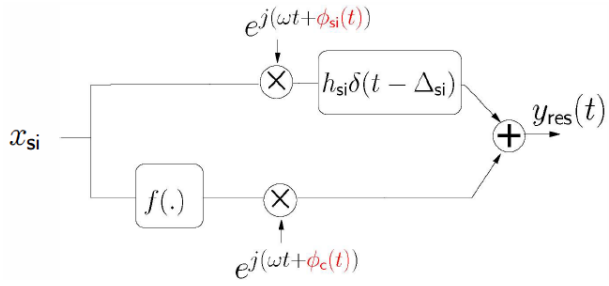

Fig. 6. Block diagram representation of the active analog canceller used in [1,2]

B. Phase noise explains the trend of cancelation

The amount of cancellation measured, when Wireless Open-Access Research Platform Project (WARP) is used as a signal source, reduces as the delay increases and eventually settles down around 35 dB. The trend in amount of cancellation can be explained if the presence of phase noise is considered in the upconverted signal. Phase noise is the jitter in the local oscillator. If the baseband signal $x(t)$ is upconverted to a carrier frequency of w_c, then the upconverted signal $x_{up}(t) = x(t)e^{j(w_c t+\phi(t))}$, where $\phi(t)$ represents the phase noise. While downconverting a signal, phase noise can be similarly defined. The variance of phase noise is defined as $\sigma_\phi^2 = \mathbb{E}(|\phi(t)|^2)$ and its autocorrelation function is denoted by $R_\phi(\cdot)$. For a measurement equipment like Vector Signal Analyser (VSA), the phase noise at the receiver is small. Therefore the total phase noise in the received signal, after downconversion, is dominated by phase noise at transmitter, i.e., the source of the signal. In presence of phase noise, the equations (5) and (6) can be rewritten as

$$y_1[iT] = h_1 e^{-j(w_c+w)\Delta_1} e^{j\phi[iT-\Delta_1]} x[iT] + z_1[iT] \quad (10)$$
$$y_2[iT] = h_2 e^{-j(w_c+w)\Delta_2} e^{j\phi[iT-\Delta_2]} x[iT] + z_2[iT] \quad (11)$$

The residual self-interference will be

$$y_{res,d}[iT] \approx jh_1 x[iT] e^{-j(w_c+w)\Delta_1}(\phi[iT-\Delta_1] - \phi[iT-\Delta_2-dT]) + z_1[iT] - z_2[(i-d)T], \quad (12)$$

V. Active Analog Cancelation

Let the phase noise in the upconvertors in the selfinterference path and the cancelling path be denoted by $\phi_{si}(t)$ and $\phi_c(t)$. Since both $\phi_{si}(t)$ and $\phi_c(t)$ are phase noises in the upconverting paths, therefore we assume $\mathbb{E}(|\phi_{si}[t]|^2) = \mathbb{E}(|\phi_c[t]|^2)$. The phase noise at the receiver downconvertor is given by $\phi_d(t)$, whose variance is given by σ_d^2. The functions $\phi_{si}(t)$ can be correlated to $\phi_c(t)$, but are independent of $\phi_d(t)$. In Fig. 5, a block diagram is shown to representat the active analog canceller used in [1, 2]. The impulse response of the over-the-air channel is $h_{si}\delta(t-\Delta_{si})$. In [1, 2], the cancelling signal is generated by processing the self-interference signal in baseband prior to upconversion, which is captured by the function $f(\cdot)$ shown in Fig. 3. Note that the local oscillator in the cancelling path is independent of the local oscillator in self-interference path, as is the case in [1, 2], thus the phase noises $\phi_{si}(t)$ and $\phi_c(t)$ are independent. The objective of the active analog canceller is to create a null for the self-interference. If the cancelling filter $f(t) = -h_{si}e^{-jw\Delta_{si}}\delta(t-\Delta_{si})$ then the cancelling signal is $x_c(t) = -h_{si}e^{-jw\Delta_{si}}x_{si}(t-\Delta_{si})$. After upconversion, the cancelling signal is given by $x_c(t)e^{j(w_c t+\phi_c(t))}$ and once the cancelling signal is added to the received self-interference signal, then the residual self-interference is given by

$$y_{res}(t) = h_{si}e^{jw_c(t-\Delta_{si})}x_{si}(t-\Delta_{si})(e^{j\phi_s(t-\Delta_{si})} - e^{j\phi_c(t)}) + z(t) \quad (13)$$

In the absence of phase noise, the residual self-interference in (11) will be only due to receiver thermal noise, which would imply a perfect null for the self-interference signal. However, the presence of phase noise results in an imperfect null. The strength of the residual self-interference signal can be estimated as

$$\mathbb{E}(|y_{res}(t)|^2) \overset{(a)}{\approx} |h_{si}|^2\,\mathbb{E}(|\phi_{si}(t-\Delta_{si}) - \phi_c(t)|^2) + \sigma_z^2 \quad (14)$$

$$\overset{(b)}{=} 2|h_{si}|^2\sigma_{si}^2 + \sigma_z^2 \quad (15)$$

where (a) holds because $\phi_{si}(t) \ll 1$,$\phi_c(t) \ll 1$, and (b) is true since the phase noise in self-interference path and cancelling path are independent. The amount of cancellation is the ratio of the strength of self-interference before cancellation to the strength of self-interference after cancellation which is $\frac{|h_{si}^2}{2|h_{si}^2\sigma_\phi^2+\sigma_z^2} \leq \frac{1}{2\sigma_\phi^2}$. The amount of active analog cancellation as a function of phase noise variance shows that reducing phase noise in local oscillator (LO) can significantly improve the amount of active analog cancellation.

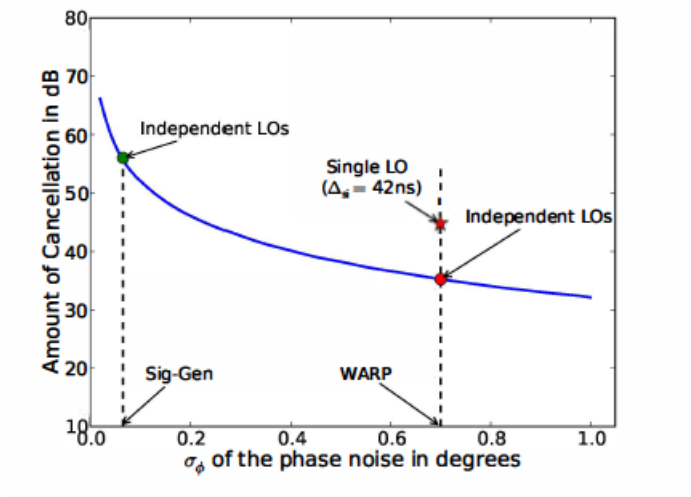

Fig. 7. Amount of active analog cancellation as a function of the variance of phase noise. The solid curve denotes the function $20log_{10}(1/2\sigma_\phi^2)$ [5]

In an alternate design, a single local oscillator can up-convert both the self-interference signal and the cancelling signal. The block diagram of an active analog canceller with a single local oscillator is shown in Fig. 8. Assuming perfect knowledge of the self-interference channel, the residual self-interference is

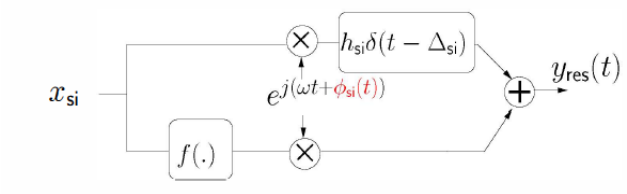

Fig. 8. Active analog canceller with matched local oscillator [4]

$$y_{res}(t) = h_{si}e^{jw_c(t-\Delta_{si})}x_{si}(t-\Delta_{si})(\phi_{si}(t-\Delta_{si}) - \phi_{si}(t)) + z(t) \quad (16)$$

and the strength of the residual self-interference is

$$\mathbb{E}(|y_{res,d}[iT]|^2) \approx 2|h_{si}|^2\sigma_\phi^2(1-R_\phi(\Delta_{si})) + 2\sigma_z^2 \quad (17)$$

In (16), the phase noises in the self-interference path and cancelling path go through different delays, thus resulting in an imperfect null for the self-interference signal. The amount of active analog cancellation can be bounded above as $\frac{|h_{si}|^2}{2|h_{si}|^2\sigma_{si}^2(1-R_\phi(\Delta_{si}))+\sigma_z^2} \leq \frac{1}{2\sigma_{si}^2(1-R_{\phi_{si}}(\Delta_{si})}$ correlation in phase noise aids in reducmg the strength of the residual, thereby increasing the amount of cancellation compared to the case when the local oscillators are independent. Therefore The amount of active analog cancellation in [1, 2] limited by the inverse of phase noise variance.

VI. Digital Cancelation

The sum total of the amount of cancellation, for serially concatenated active analog and digital stages of cancellation, is bounded above by the inverse of the variance of phase noise of the local oscillators. Here designs of active analog cancellers with independent local oscillators in self-interference and cancelling paths is considered. However, the arguments easily extend to designs with a single local oscillator. The digital canceller operates on the residual self-interference after active analog cancellation. If the active analog canceller has perfect knowledge of the self-interference channel, then the residual self-interference after active analog cancellation is given by (13), which after down conversion can be approximated as

$$y_{res}(iT) = h_{si}e^{jw(t-\Delta_{si})}x_{si}(iT-\Delta_{si})(\phi_{si}(iT-\Delta_{si}) - \phi_c(iT)) + z(iT) \quad (18)$$

From (18), it is noted that the residual self-interference is a noisy version of the self-interference signal multiplied with function of phase noise. Since phase noise is unknown and changes every sample, $y_{res}(iT)$ can be seen as a fast-fading version of the self-interference signal. The correlation of $y_{res}(iT)$, with the self-interference signal itself is approximately zero because phase noise is zero mean and independent of the self-interference signal. Thus, if perfect knowledge of self-interference channel is available, then after active analog cancellation the residual self-interference signal is not correlated to the self-interference signal and hence the digital canceller does not reduce the self-interference at all.

Digital cancellation will help cancel self-interference only when the self-interference channel is not known perfectly. As an example, assume that there is a slight error in the knowledge of the delay of the self-interference channel. Let $\hat{\boldsymbol{h}}_{si}(t) = \hat{h}_{si}(t-\tau)$, where $(\Delta_{si} - \tau)$ denotes the error in

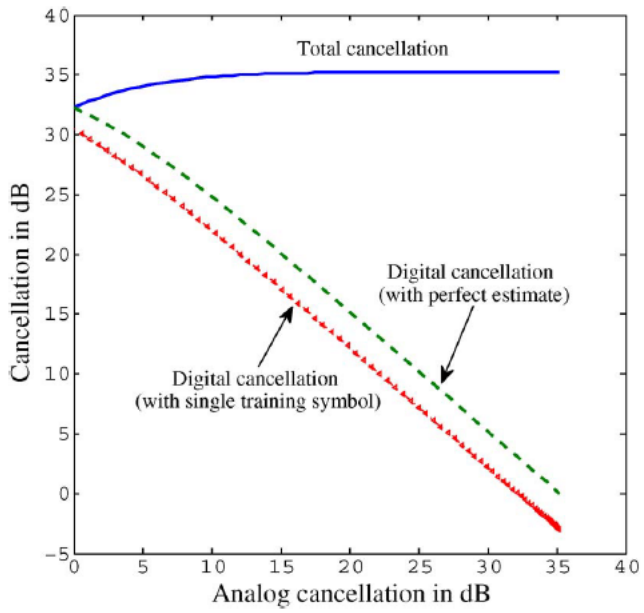

Fig. 9. Relationship between amount of active analog cancelation and the amount of digital cancelation [5]

the knowledge of delay. Then, the residual self-interference in digital baseband is given by

$$y_{res}(iT) \approx h_{si}e^{-j(w\Delta_{si}+\phi_c[iT]-\phi_d[iT])}(x_{si}[iT-\Delta_{si}]- x_{si}[iT-\tau]t + x_{si}[iT-\Delta_{si}](\phi_{si}[iT-\Delta_{si}- \phi_c(iT)) + z(iT) \quad (19)$$

The strength of the residual self-interference before digital cancellation is $2|h_{si}|^2(1-R_x(\Delta_{si})+\tau)+\sigma_z^2$. The digital canceller can reduce the self-interference by using $-h_{si}e^{-jw\Delta_{si}}(x_{si}[iT-\Delta_{si}]-x_{si}[iT-\tau])$as the cancelling signal. After digital cancellation, the strength of residual self-interference is $2|h_{si}|^2((1-R_x(\Delta_{si}-\tau))+(\sigma_{si}^2+\sigma_d^2)+\sigma_\phi^2)+\sigma_z^2$. Since the variance of phase noise is much smaller than unity, the digital canceller can reduce the strength of the residual self-interference by choosing appropriate cancelling signal. However, it is noted that even after digital cancellation the strength of the residual self-interference is lower bounded by $2|h_{si}|^2\sigma_{si}^2+\sigma_z^2$, which is the strength of residual self-interference signal if the estimation error is zero. Digital cancellation manages to cancel only the part of the residual self-interference which is correlated to the selfinterference signal itself. The sum total of active analog and digital cancellation is upper bounded by $\frac{1}{2\sigma_{si}^2}$. Thus, as the amount of active analog cancellation increases, the amount of digital cancellation deteriorates.

VII. Influence of Passive Suppression on Active Cancelation

In this section the following question is answered : "How and when does passive suppression impact the amount of analog cancelation?"

Let us consider a self-interference channel with two nonzero taps, which can be considered as taps representing the line-of-sight and reflected components. Let the two-tap self-interference channel be $\boldsymbol{h}_{si}(t)=h_1\delta(t-\Delta_1)+h_2\delta(t-\Delta_2)$, where Δ_1 and $\Delta_1$denote the delays of the line-of- sight and reflected components; therefore, $\Delta_1<\Delta_2$. The average strength of the line-of-sight and reflected components is captured by $\mathbb{E}(|h_1|^2)$ and $\mathbb{E}(|h_2|^2)$. From experimental observations, it is reasonable to assume that passive suppression can reduce the strength of the line-of-sight component. Therefore, the amount of passive suppression determines the ratio $\mathbb{E}(|h_1|^2)/\mathbb{E}(|h_2|^2)$.

Assume that the self-interference channel is perfectly known. Then, the canceling signal in baseband is

$$x_{cancel}(t) = -h_1x_{si}(t-\Delta_1)e^{-jw_c\Delta_1}-h_2x_{si}(t-\Delta_2)e^{-jw_c\Delta_2} \quad (20)$$

In presence of phase noise, the residual self-interference is

$$\begin{aligned} y_{residual}(t) &= -h_1x_{si}(t-\Delta_1)e^{-jw_c\Delta_1}(e^{j\phi(t-\Delta_1)}-e^{j\phi(t)}) \\ &+ h_2x_{si}(t-\Delta_2)e^{-jw_c\Delta_2}(e^{j\phi(t-\Delta_2)}-e^{j\phi(t)}) \\ &+ z_{noise}(t) \\ &\approx jh_1x_{si}(t-\Delta_1)e^{-jw_c\Delta_1}(\phi(t-\Delta_1)-\phi(t)) \\ &+ jh_2x_{si}(t-\Delta_2)e^{-jw_c\Delta_2}(\phi(t-\Delta_2)-\phi(t)) \\ &+ z_{noise}(t) \end{aligned}$$

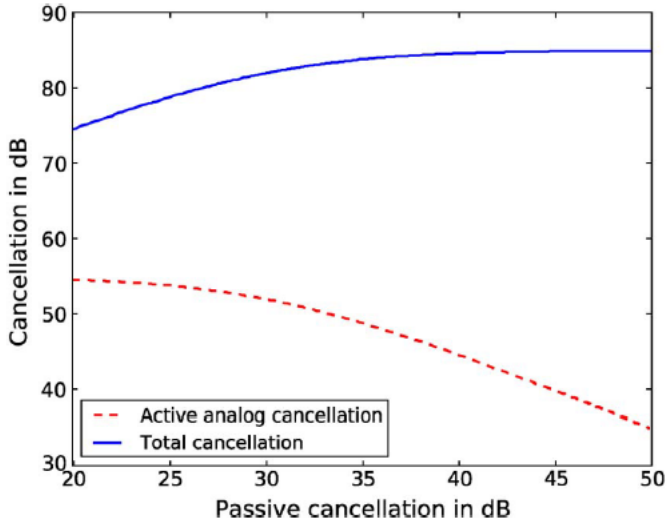

Fig. 10. Total cancelation represents the sum of passive and active analog cancelation when operated in cascade [5]

The strength of the residual signal is

$$\mathbb{E}(|y_{residual}(t)|^2) \quad (21)$$

$$2\,\mathbb{E}(|h_1|^2)(1-R_{\phi_{si}}(\Delta_1))$$

$$2\,\mathbb{E}(|h_2||^2)(1-R_{\phi_{si}}(\Delta_2))$$

$$2\,\mathbb{E}(Re(h_1h_2'x_{si}(t-\Delta_1)x_{si}'(t-\Delta_2) \quad (22)$$

$$e^{jw_c}(\Delta_2-\Delta_1)))(1+R_{\phi_{si}}(\Delta_1-\Delta_2)$$

$$-R_{\phi_{si}}(\Delta_1)-R_{\phi_{si}}(\Delta_2))\sigma_\phi^2 \quad (23)$$

Thus, higher passive suppression can result in lower active analog cancelation in pre-mixer cancelers. However, increasing passive suppression implies that the sum of cascaded passive and active analog cancelation increases.

VIII. Signal Model for full-Duplex

Using the analyses in Sections V and VI, a signal model is developed for single-input?single-output (SISO) full-duplex communication and then extend it to the MIMO and wideband cases.

A. Narrowband Signal Model

In this section, a digital baseband signal model is presented, that captures the effect of phase noise and imperfection in channel estimates by considering the residual self-interference after 1) active analog cancelation and 2) digital cancelation cascaded with active analog cancelation.

1) Active Analog Cancelation with imperfect estimates: For pre-mixer cancelers, the residual self-interference is given by (59). Since phase noise is assumed to be zero-mean Gaussian, the linear combination of several phase noise terms is also Gaussian. In addition, phase noise is assumed to be small; therefore, $e^{j(\phi_{si}(t-\Delta_{si})-\phi_{cancel}(t))} \approx 1$. Then, the received signal at N1, which is a combination of residual self-interference, signal of interest, and thermal noise, can be written as

$$\begin{aligned} y_1[iT] =& \sqrt{P_{signal}}\boldsymbol{h}_{signal}[iT] * x_{signal}[iT] \\ &+ \sqrt{P_{si}}|h_{si}|\beta_\phi z_{phase-noise}[iT] \\ &+ \sqrt{P_{si}}h_{residual-si}[iT] * x_{si}[iT] + z_{noise}[iT] \end{aligned} \tag{24}$$

where $z_{phasenoise}[iT]$ is the zero-mean additive white Gaussian noise with unit variance independent of the thermal noise and signal of interest. Signal $x_{signal}[iT]$ is of unit variance, and P_{si} and P_{signal} are power constraints at N_1 and N_2, respectively.

2) Imperfect estimates in active analog and digital cancelation: After digital cancelation, the residual depends on the quality of the estimate of residual self-interference channel, in addition to phase noise. The received signal at N1 is given as

$$\begin{aligned} y_1[iT] =& \sqrt{P_{signal}}\boldsymbol{h}_{signal}[iT] * x_{signal}[iT] \\ &+ \sqrt{P_{si}}|h_{si}|\gamma_\phi z_{phase-noise}[iT] \\ &+ \sqrt{P_{si}}\left(h_{residual-si}[iT] - \hat{h}_{residual-si}[iT]\right) * x_{si}[iT] \\ &+ z_{noise}[iT] \end{aligned} \tag{25}$$

where γ_ϕ is a parameter dependent on the phase noise and the quality of active analog cancelation.

B. Wideband Signal Model

In wideband full-duplex, the self-interference channel need not be frequency flat [13]. A wideband signal model is proposed for full-duplex by considering the bandwidth to be a combination of several narrowband full-duplex systems. If the overall bandwidth of the wideband system $W \ll w_c$, then the phase jitter over the band of interest can be assumed to be independent of the bandwidth [13]. Assuming W to be a combination of K narrowbands, we arrive at the full-duplex signal model after active cancelation in the k^{th} band, i.e., $k = 1, 2...K$, as

$$\begin{aligned} y_{1,k}[iT] =& \boldsymbol{h}_{signal,k}[iT] * x_{signal,k}[iT] \\ &+ \sqrt{P_{si,k}}|h_{si,k}|\beta_\phi z_{phase-noise,k}[iT] \\ &+ \sqrt{P_{si}}\boldsymbol{h}_{residual-si,k}[iT] * x_{si,k}[iT] + z_{noise}[iT] \end{aligned} \tag{26}$$

where $P_{si,k}$ and $|h_{si,k}|$ are the power constraint and the magnitude of the self-interference channel in the kth band respectively. To compare the bottleneck in narrowband versus wideband system, let us assume the total power in both systems is the same, say, P. As a simplifying assumption, let $|h_{si,k}| = |h_{si}|$. In the narrowband system, the strength of residual self-interference due to phase noise is $P|h_{si}|^2\beta_{phi}^2$, which is the same as the strength of the residual self-interference due to phase noise in wideband, i.e., $\sum_{i=1}^{K} P_{si,k}|h_{si}|^2\beta_{phi}^2 = P|h_{si}|^2\beta_{phi}^2$. On the other hand, if the thermal noise floor in narrowband is given by variance σ_{noise}^2, then the variance of the noise over wideband is $K\sigma_{noise}^2$. Thus, a wideband system has a relatively higher thermal noise floor, whereas the phase noise floor remains unchanged. The signal model after digital cancelation can be written by simply replacing β_ϕ with γ_ϕ, and $\boldsymbol{h}_{residual-si,k}[iT]$ with $\hat{\boldsymbol{h}}_{residual-si,k}[iT]$ in (26).

C. MIMO Full-Duplex Signal Model

To extend the narrowband SISO model (24), we assume a MIMO system withM transmit antenna and N receive antenna. The self-interference at each of the receivers is due to the sum of M transmissions: one from each transmit antenna. If the transmit radio chain for each antenna has an independent local oscillator, then the residual self-interference due to phase noise is the sum of M independent residuals due to phase noise in a SISO system. Thus the received signal after analog cancelation at the nth receiver of the full-duplex node N_1 is given as

$$\begin{aligned} y_{1,n}[iT] =& \sum_{m=1}^{M} \sqrt{P_{signal,m}}\boldsymbol{h}_{signal,mn}[iT] * x_{signal,m}[iT] \\ &+ \gamma_\phi \left(\sum_{m=1}^{M} |h_{si,m}|^2 P_{si,m}\right)^{1/2} z_{phase-noise,n}[iT] \\ &+ \sum_{m=1}^{M} \boldsymbol{h}_{residual-si,mn}[iT] * x_{si,m}[iT] \\ &+ z_{noise,n}[iT] \end{aligned} \tag{27}$$

where $z_{phase-noise,n}[iT]$ is unit variance, whereas $z_{noise,n}[iT]$ has a variance of σ_{noise}^2. The $\boldsymbol{h}_{signal,mn}[iT]$ represents the channel for the signal of interest from mth transmitter to nth receiver. The self-interference channel and the residual selfinterference channel at N1 is represented by $\boldsymbol{h}_{si,mn}[iT]$ and $\boldsymbol{h}_{residual-si,mn}[iT]$, respectively. Power

constraints at the mth transmitter for the signal of interest and self-interference is $P_{signal,m}$ and $P_{si,m}$, respectively. To qualitatively understand the MIMO model in (27), consider the special case where all the self-interference channels have identical magnitude, and the residual self-interference is simply M times the residual self-interference for SISO.

IX. Example Case: Phase noise analysis in All-Digital Self-Interference Cancellation Technique for Full-Duplex Systems

In this section, the system model of the full-duplex transceiver architecture is described in detail [9]. Fig.(10) shows a detailed block diagram for the proposed digital self-interference cancellation technique based on a new full-duplex transceiver architecture. The transceiver consists of the ordinary transmit and receive chains in addition to one auxiliary receiver chain used for self-interference cancellation. At the transmitter side, the information signal X is orthogonal frequency division multiplexing (OFDM) modulated, then up-converted to the RF (Radio Frequency) frequency.

A. System Model

The up-converted signal is then filtered, amplified, and transmitted through the transmit antenna. A fraction of the amplified signal is fed-back as input to the auxiliary receiver chain. The signal power at the auxiliary receiver input is controlled through the power splitter; therefore, the low noise amplifier (LNA) is omitted from the auxiliary receiver chain. The feed-back and ordinary-received signals are down-converted to base-band through the auxiliary and ordinary receiver chains, respectively. The auxiliary and ordinary receiver chains are identical and share the same phase locked loop (PLL). The channel transfer function H^{aux} is the frequency domain representation of the wired channel from the power amplifier (PA) output to the auxiliary receiver. The channel transfer function H^{ord} is the frequency-domain representation of the self-interference wireless channel. In this paper, upper-case letters represent frequency-domain signals and lower-case letters represent time-domain signals.

The output of the auxiliary and the ordinary receiver chains are fed to a channel estimation block to obtain an estimate for the ratio between the ordinary and auxiliary channels (H^{ord}/H^{aux}). The channel estimation process is performed using time-orthogonal training sequences transmitted at the beginning of each data frame. The estimated channel is then multiplied with the auxiliary receiver output, and the multiplication output is subtracted from the received signal to obtain an interference-free signal.

In this study, the main transmitter and receiver impairments are considered. More specifically, transmitter and receiver phase noise, transmitter and receiver nonlinearities, analog-to- digital converter (ADC) quantization noise, and receiver Gaussian noise. Since the feed-back signal is obtained from the PA output which contains a copy of the transmitter impairments, the proposed architecture can significantly mitigate all transmitter impairments. In addition, the receiver phase noise effect is mitigated by means of sharing the same PLL between the auxiliary and ordinary receiver chains.

In the presence of the transmitter phase noise ϕ^{tx} and the PA nonlinear distortion signal d^{tx}, the transmitted signal at the PA output can be written as

$$y^{tx}(t) = x(t)e^{j(2\pi f_c t + \phi^{tx}}(t)) + d^{tx}(t) \tag{28}$$

where x is the transmitter base-band signal, d^{tx} is the transmitter nonlinear distortion due to the PA, and f_c is the carrier frequency. At the auxiliary receiver output, the digital baseband signal y^{aux} can be written as

$$y_n^{aux} = \left(y_n^{tx} * h_n^{aux}\right) e^{j\phi_n^{tx}} + q_n^{aux} + z_n^{aux} \tag{29}$$

where $*$ denotes convolution process, n is the sample index, y_n^{tx} is the digital base-band representation of $y^{tx}(t)$, h^{aux} is the wired channel from the PA output to the auxiliary receiver input, ϕ^{rx} is the receiver phase noise process, q^{aux} is the auxiliary receiver ADC quantization noise, and z^{aux} is the auxiliary receiver Gaussian noise. Similarly, the digital base-band signal y^{ord} at the ordinary receiver output can be written as

$$y_n^{ord} = \left(y_n^{tx} * h_n^{ord}\right) e^{j\phi_n^{tx}} + d_n^{rx} + q_n^{ord} + z_n^{ord} + s_n^{soi} \tag{30}$$

where superscript ord refers to the ordinary receiver chain signals, d^{rx} is the receiver nonlinear distortion due to the LNA, and s^{soi} is the received signal-of-interest (including the signal-of-interest channel and all impairments). After digial self-interference cancellation, the the post-cancellation signal Y^{DC} can be written as

$$Y_k^{DC} = Y_k^{ord} - Y_k^{aux}\hat{H}_k \tag{31}$$

where uppercase letters denote the frequency domain representation of the corresponding signals, k is the subcarrier index, and $\hat{H}$ is an estimate for the ratio between the ordinary and auxiliary channels (H^{ord}/H_{aux}) calculated in the least square (LS) form as

$$\hat{H}_k = \frac{Y_k^{ord}}{Y_k^{aux}} \tag{32}$$

For a complete signal model, a detailed description for the impairments and channel modeling is presented in the following subsections.

1) Transceiver Phase Noise: Generally, modeling the phase noise process depends on the oscillator type. There are two main oscillator types: freerunning oscillators and PLL based oscillators. In free-running oscillators the phase noise could be modeled as a Wiener process, where the phase error at the nth sample is related to the previous one as $\phi_n = \phi_{n-1} + \beta$, where β is a Gaussian random variable with zero mean and variance $\sigma^2 = 4\pi f_{3dB} T_s$. In this notation T_s describes the sample interval and f_{3dB} is the 3 dB bandwidth of the phase noise Lorentzian spectrum.

In PLL based oscillators, as shown in Fig. 11, the voltage controlled oscillator (VCO) output is controlled through a

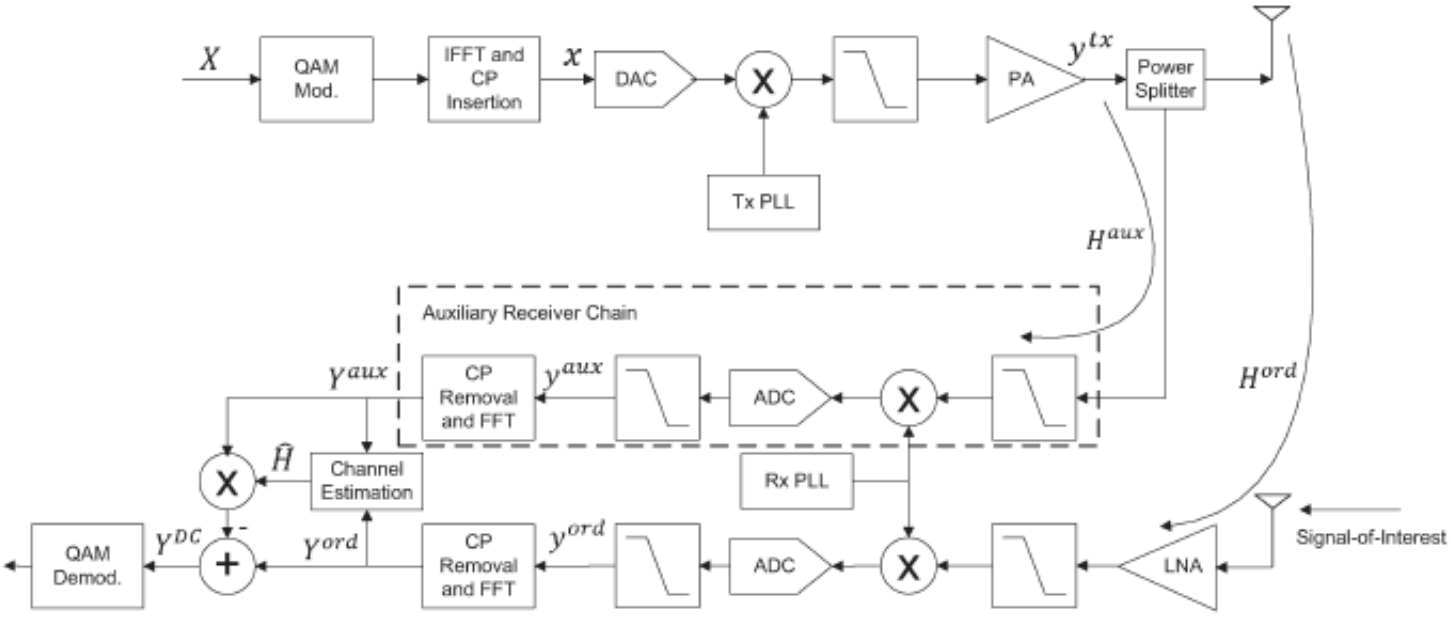

Fig. 11. Detailed block diagram for the proposed digital self-interference cancellation technique [9]

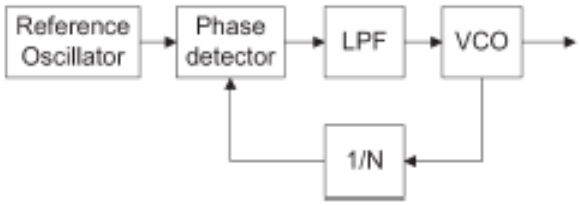

Fig. 12. Block diagram for a PLL based oscillator [9]

feedback loop that involves a phase detector and low-pass filter (LPF). The purpose of the feed-back loop is to lock the phase of the VCO output with the phase of a high quality reference oscillator. The PLL output phase noise can be modeled as Ornstein-Uhlenbeck process with auto-correlation function calculated as

$$E[e^{j\Delta\phi_{mn}}] = e^{\frac{-4\pi^2 f_c^2}{2}\left(CT_s|m-n| + 2\sum_{i=0}^{n_0}(\mu_i+v_i)(1-e^{-\lambda_i T_s|m-n|}\right)} \quad (33)$$

where (n_0, μ, v, λ) are PLL specific parameters that are function of the PLL loop filter design. The power spectral density (PSD) of the PLL phase noise is obtained by taking the Fourier transform of equation (33). Since PLL-based oscillators are commonly used in wireless systems, the numerical analysis in this paper is performed using PLL-based oscillators.

B. Self-Interference Cancelation Analysis

The main idea of the cancellation technique is to obtain a copy of the transmitted self-interference signal including all transmitter impairments, and use this copy for digital-domain self-interference cancellation at the receiver side. Hypothetically speaking, if both auxiliary and ordinary receiver chains are impairment-free, the architecture should be able to totally eliminate both the self-interference signal and the transmitter impairments. However, due to the receiver impairments and the channel estimation errors, perfect self-interference cancellation is not possible. In fact, receiver impairments and channel estimation errors introduce certain limitations on the self-interference cancellation capability. To understand these limitations, we analytically and numerically investigate the impact of the receiver impairments and channel estimation errors on the self-interference cancellation capability of the proposed technique.

1) Impact of Receiver Phase Noise: In this analysis, the receiver is assumed to have only the phase noise impairment. Furthermore, the auxiliary and ordinary receiver chains are sharing the same PLL, and thus have the same phase noise signal. In the presence of only receiver phase noise, the auxiliary and ordinary receiver outputs (Equation (29) and (30)) can be rewritten as

$$y_n^{aux} = \left(y_n^{tx} * h_n^{aux}\right) e^{j\phi_n^{rx}} \quad (34)$$

$$y_n^{ord} = \left(y_n^{tx} * h_n^{ord}\right) e^{j\phi_n^{rx}} + s_n^{soi} \quad (35)$$

By performing Discrete Fourier Transform (DFT), the frequency domain representation of (34) and (35) can be written

as

$$Y_k^{aux} = \sum_{l=0}^{N-1} Y_l^{tx} H_l^{aux} J_{k-1}^{rx} \tag{36}$$

$$Y_k^{ord} = \sum_{l=0}^{N-1} Y_l^{tx} H_l^{ord} J_{k-1}^{rx} + S_k^{soi} \tag{37}$$

where N is the number of subcarriers per OFDM symbol, and J^{rx} is the DFT coefficients of the phase noise process $e^{j\phi^{rx}}$ calculated as

$$J_k^{rx} = \sum_{n=0}^{N-1} e^{j\phi_n^{rx}} e^{-j2\pi nk/N} \tag{38}$$

Since H^{aux} is a wired channel, it can be assumed that H^{aux} has a frequency flat response. Accordingly, equation (36) can be simplified as

$$Y_k^{aux} = H_k^{aux} \sum_{l=0}^{N-1} Y_l^{tx} J_{k-1}^{rx} \tag{39}$$

After self-interference cancellation, the post-cancellation signal Y^{DC} can be written as

$$Y_k^{DC} = S_k^{soi} + \sum_{l=0}^{N-1} \left(H_l^{ord} - H_k^{ord}\right) Y_l^{tx} J_{k-1}^{rx} \tag{40}$$

The second term in the right hand side of (40) represents the residual self-interference signal due to the receiver phase noise effect. According to (40), the simplified residual self-interference (RSI) power PRSI can be calculated as

$$P_{RSI} = P^{tx} E\left[\left|\sum_{l=0, l\neq k} (H_l^{ord} - H_k^{ord})\right|^2\right] E\left[\left|J_{k-1}^{rx}\right|^2\right] \tag{41}$$

An upper bound for the residual self-interference power is obtained when $H_k^{ord,nlos}$ and $H_l^{ord,nlos}$ are uncorrelated for all $k \neq l$. On the other hand, it is obvious that the lower bound of the residual self-interference power is zero. The lower bound is achieved when the self-interference channel has frequency-flat transfer function. Between the upper and lower bounds, the residual self-interference power is determined by the self-interference channel characteristics, mainly the correlation between the channel frequency response at different subcarriers.

To quantify the phase noise mitigation gain achieved due to the coherence bandwidth (CBW) of the channel, the system is simulated under three different channel models with different maximum delay spread (i.e., different CBW). The simulated channel models are the 'B', 'C', and 'D' TGn channel models. Residual self-interference power due to receiver phase noise effect for different channel models with -40 dBc total in-band phase noise power. The 'B', 'C', and 'D' channel models have a maximum delay spread of 80, 200, and 390ns, respectively. Fig.12 shows the residual self-interference power

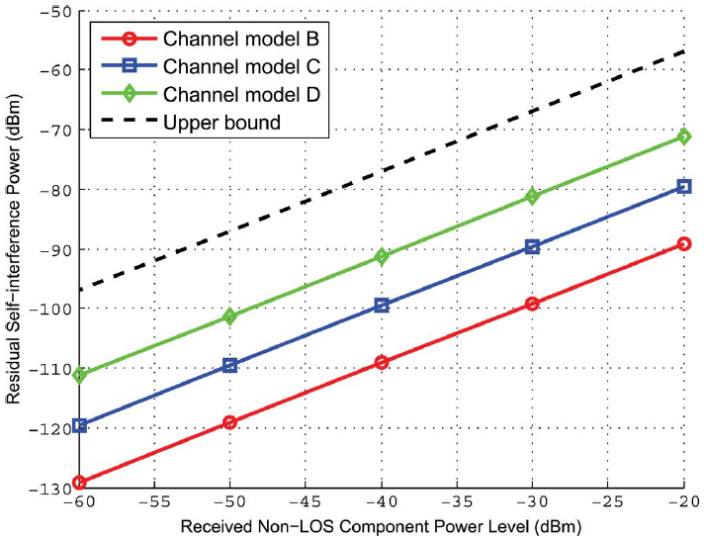

Fig. 13. Residual self-interference power due to receiver phase noise effect for different channel models with -40 dBc total in-band phase noise power. [9]

for the three channel models at different non-LOS(Line-of-Sight) component power levels, with total phase noise power of -40 dBc. The results show that, larger CBW results in lower residual self-interference power (i.e., more phase noise mitigation). In terms of numbers, approximately 15-30 dB reduction in residual self-interference power compared to the upper bound is achieved due to the correlation between the channel frequency responses within the CBW of the channel.

X. Conclusion

This study has provided an analytical explanation of experimentally observed performance bottlenecks in full-duplex systems. The analysis clearly answers all the questions posed by self-interference cancelation and shows that phase noise is a major bottleneck in current full-duplex systems and thus reducing the phase noise figure of radio mixers could lead to improved self-interference cancelation.

In the example case, a novel all-digital self-interference cancellation technique for full-duplex systems is studied. This technique uses an auxiliary receiver chain to obtain a digital-domain copy of the transmitted RF self-interference signal including all transmitter impairments. The self-interference signal copy is then used in the digital-domain to cancel out both the self-interference signal and the transmitter impairments. To alleviate the receiver phase noise effect, a common oscillator is shared between the auxiliary and ordinary receiver chains. A thorough analytical and numerical analysis for the effect of the transmitter and receiver impairments on the cancellation capability of the technique is presented. The analyses show that the technique used significantly mitigates the transceiver phase noise. Also a possible extension to this work would be deploying this architecture in MIMO full-duplex systems with detailed investigation of the achievable gains.

REFERENCES

[1] M. Duarte and A. Sabharwal, *"Full-Duplex Wireless Communications Using Off-The-Shelf Radios: Feasibility and First Results,"* in Proceedings of Asilomar Conference on Signals. Syslems and Computers, 2010.

[2] M. Duarte, C. Dick and A. Sabharwal, *"Experiment-Driven Characterization of Full-Duplex Wireless Systems,"* in IEEE Transactions on Wireless Communications, vol. 11, no. 12, pp. 4296-4307, December 2012.

[3] Ashutosh Sabharwal et al.,*"In-Band Full-Duplex Wireless: Challenges and Opportunities"*, IEEE Journal on Selected Areas on Communications, vol.32,no.9,pp.1637-1651,Sep 2014

[4] A. Sahai, G. Patel, C. Dick, and A. Sabharwal, *"Understanding the impact of phase noise on active cancellation in wireless full-duplex,"* in Proc. 2012 ,Asilomar Conf. Signals, Syst., Comput.

[5] A. Sahai, G. Patel, C. Dick, and A. Sabharwal, *"On the impact of phase noise on active cancellation in wireless full-duplex,"* IEEE Trans. Veh.Technol., vol. 62, no. 9, Nov. 2013.

[6] Elsayed Ahmed,Ahmed M. Eltawil,Ashutosh Sabharwal,*"Self-Interference Cancellation with Phase Noise Induced ICI Suppression for Full-Duplex Systems,"* in Proc Globecom 2013 - Signal Processing for Communications Symposium

[7] E. Ahmed, A. M. Eltawil and A. Sabharwal,*"Self-interference cancellation with nonlinear distortion suppression for full-duplex systems,"* 2013 Asilomar Conference on Signals, Systems and Computers, Pacific Grove, CA, 2013, pp. 1199-1203.

[8] Elsayed Ahmed and Ahmed M. Eltawil,*"On Phase Noise Suppression in Full-Duplex Systems,"* IEEE Trans. on Wireless Communications, vol. 14, no.3 ,Mar 2015

[9] Elsayed Ahmed and Ahmed M. Eltawil,*"All-Digital Self-Interference Cancellation Technique for Full-Duplex Systems,"* IEEE Trans. on Wireless Communications, vol. 14, no. 7, July 2015

[10] V. Syrjala, M. Valkama, L. Anttila, T. Riihonen, and D. Korpi, *"Analysis of oscillator phase-noise effects on self-interference cancellation in full-duplex OFDM radio transceivers,"* IEEE Trans. Wireless Commun., vol. 13, no. 6, pp. 2977-2990, Jun. 2014

[11] Z. Zhang, K. Long, A. V. Vasilakos and L. Hanzo,*"Full-Duplex Wireless Communications: Challenges, Solutions, and Future Research Directions,"* in Proceedings of the IEEE, vol. 104, no. 7, pp. 1369-1409, July 2016.

[12] P. Robertson and S. Kaiser, *"Analysis of the effects of phase-noise in orthogonal frequency division multiplex (OFDM) systems,"* in Proc. 1995 IEEE International Conf. Commun., vol. 3, pp. 1652-1657.

[13] E. Everett, M. Duarte, C. Dick, and A. Sabharwal, *"Empowering full-duplex wireless communication by exploiting directional diversity,"* in Proc. Asilomar Conf. Signals, Syst. Comput., 2011, pp. 2002-2006.